Bipolar Tetraether Lipids: Chain Flexibility and Membrane Polarity Gradients from Spin-Label Electron Spin Resonance

R. Bartucci,*,‡ A. Gambacorta,§ A. Gliozzi,|| D. Marsh,⊥ and L. Sportelli‡

Dipartimento di Fisica, Università della Calabria, I-87036 Arcavacata di Rende (CS), Italy, Istituto di Chimica Biomolecolare, Consiglio Nazionale delle Ricerche, I-80078 Pozzuoli (NA), Italy, Dipartimento di Fisica, Università di Genova, I-16146 Genova, Italy, and Max-Planck-Institut fur Biophysikalische Chemie, D-37077 Gottingen, Germany

Received June 9, 2005; Revised Manuscript Received September 16, 2005

ABSTRACT: Membranes of thermophilic Archaea are composed of unique tetraether lipids in which C40, saturated, methyl-branched biphytanyl chains are linked at both ends to polar groups. In this paper, membranes composed of bipolar lipids P2 extracted from the acidothermophile archaeon *Sulfolobus solfataricus* are studied. The biophysical basis for the membrane formation and thermal stability is investigated by using electron spin resonance (ESR) of spin-labeled lipids. Spectral anisotropy and isotropic hyperfine couplings are used to determine the chain flexibility and polarity gradients, respectively. For comparison, similar measurements have been carried out on aqueous dispersions of diacyl reference lipid dipalmitoyl phosphatidylcholine and also of diphytanoyl phosphatidylcholine, which has methyl-branched chains. At a given temperature, the bolaform lipid chains are more ordered and less flexible than in normal bilayer membranes. Only at elevated temperatures (80 °C) does the flexibility of the chain environment in tetraether lipid assemblies approach that of fluid bilayer membranes. The height of the hydrophobic barrier formed by a monolayer of archaebacterial lipids is similar to that in conventional fluid bilayer membranes, and the permeability barrier width is comparable to that formed by a bilayer of C16 lipid chains. At a mole ratio of 1:2, the tetraether P2 lipids mix well with dipalmitoyl phosphatidylcholine lipids and stabilize conventional bilayer membranes. The biological as well as the biotechnological relevance of the results is discussed.

The membrane lipids of the Archaea, in contrast to those of eukaryotes and bacteria, have *sn*-2,3 ether-linked chains that are fully saturated but contain branched methyl groups (*1*, *2*). Of these, the thermoacidophilic archaeal species, which live in extreme environments of low pH and high temperature, are characterized by tetraether lipids of unique cyclic structure. In addition to imparting the necessary mechanical and thermal stability to the membranes of the native organism, the isopranyl tetraether lipids are also capable of stabilizing vesicles formed by conventional diacyl phospholipids, which opens up the possibility of biotechnological applications (*3*).

Different physicochemical properties such as structure, dynamics, polymorphism, and thermal and mechanical stability of bipolar lipid fractions extracted from thermoacidophilic archaebacteria have been investigated in several experimental works (*4*−*15*). In particular, by means of two-photon fluorescence microscopy (*11*) and perylene fluorescence spectroscopy (*12*), a rigid and tight membrane packing has been evidenced in liposomes of polar lipid fraction E (PLFE) from *Sulfolobus acidocaldarius*. Moreover, the motion of three spin label positional isomers of stearic acid (*n*-SASL, $n = 5$, 12, and 16) in the hydrolytic lipid fractions glycerol-dialkyl-glycero-tetraether (GDGT)[1] and glycerol-dialkyl-nonitol-tetraether (GDNT) from *Sulfolobus solfataricus* is restricted in the time scale of both conventional and saturation-transfer electron spin resonance (ESR) spectroscopy (*5*). In these systems, an appreciable fluidity is gained only at temperatures close to the minimum growth temperature of the respective thermoacidophilic archaebacteria (*5*, *11*, *12*).

Virtually all membrane lipids of the acidothermophile archaeon *S. solfataricus* consist of two C_{40} $\omega-\omega'$ biphytanyl residues, with 0−4 cyclopentane groups/chain, that are ether-linked at both ends to glycerol or nonitol groups (*6*). The P2 hydrolytic lipid fraction from this archaeon is the most abundant of the polar lipids extracted from the plasma membrane and is composed of ca. 90% of a glycerol−nonitol lipid (GDNT) and 10% of a glycerol−glycerol lipid (GDGT, see Figure 1). Both polyols are substituted with hydrophilic moieties, leading to a lipid with two polar "headgroups", one at each end of the molecule. This P2-lipid fraction has been found to generate solely lamellar lyotropic phases in

* To whom correspondence should be addressed. Telephone: +39-0984-496074. Fax: +39-0984-494401. E-mail: bartucci@fis.unical.it.
‡ Università della Calabria.
§ Consiglio Nazionale delle Ricerche.
|| Università di Genova.
⊥ Max-Planck-Institut fur Biophysikalische Chemie.

[1] Abbreviations: DPPC, 1,2-dipalmitoyl-*sn*-glycero-3-phosphocholine; DPhPC, 1,2-diphytanoyl-*sn*-glycero-3-phosphocholine; GDGT, glycerol dialkylglycerol tetraether lipid; GDNT: glycerol dialkylnonitol tetraether lipid; *n*-PCSL, 1-palmitoyl-2-[*n*-(4,4-dimethyl-oxazolidin-*N*-oxyl)stearoyl]-*sn*-glycero-3-phosphatidylcholine; ESR, electron spin resonance.

10.1021/bi051101i CCC: $30.25
Published on Web 10/22/2005

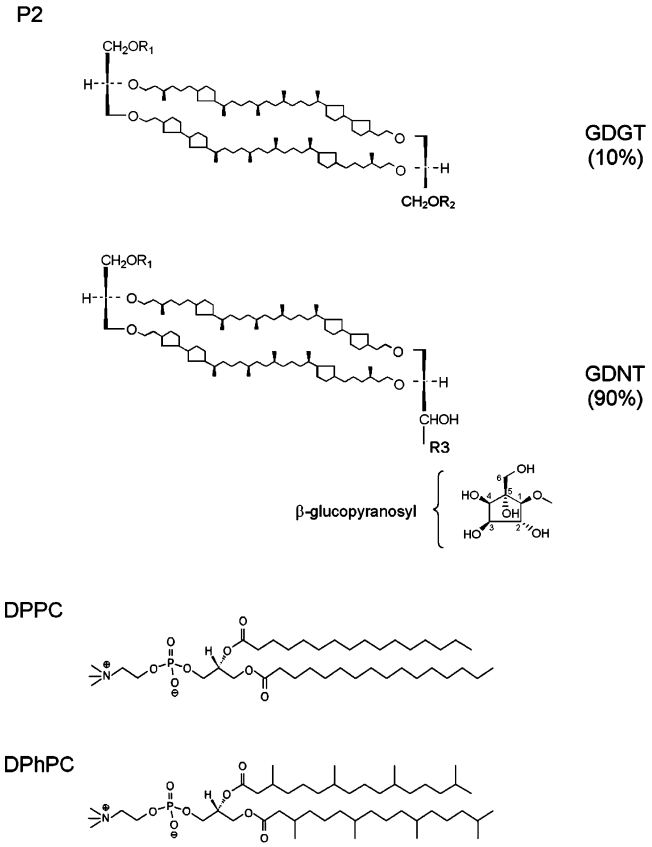

FIGURE 1: Structures of the lipid molecules used in this study. (Bipolar lipids P2) Glycerol dialkylglycerol tetraether lipid (GDGT, ≈10% of the lipid fraction) in which R1 = *P*-inositol and R2 = β-D-glucopyranosyl-β-D-galactopyranose. Glycerol dialkylnonitol tetraether lipid (GDNT, ≈90% of the lipid fraction) in which R3 is the cyclopentanoid part of the polyol to which carbon 2 or 3 is linked β-D-glucopyranosyl. Each phytanyl chain may contain up to four cyclopentane rings. The average number is 2.3. (DPPC) Synthetic zwitterionic lipid 1,2-dipalmitoyl-*sn*-glycero-3-phosphocholine. (DPhPC) Synthetic zwitterionic lipid 1,2-diphytanoyl-*sn*-glycero-3-phosphocholine.

water (*7*) and hence is an excellent object with which to study membranes composed of these bipolar, bolaform lipids.

Not all fractions of the membrane lipids of *S. solfataricus* are able to form closed amphiphilic assemblies. The conditions that lead to the formation of vesicles can be analyzed according to the theory introduced by Israelachvili (*16*). These analysis and experimental results indicate that lipids of the P2 fraction span a monolayer-type membrane with minimal contribution from bent molecules, which is very different from the usual bilayer membrane structures that are formed by monopolar diacyl lipids (*17*). It is therefore of considerable interest to investigate how the cyclic tetraether structure affects the chain mobility and flexibility and the polarity barrier of P2-lipid membranes. A related issue concerns the way in which bipolar lipids are able to stabilize conventional bilayer membranes (*8*, *16*) and to sustain a membrane barrier in the high-temperature environments of extreme thermophiles.

The aforementioned biophysical properties of model membranes composed of only bipolar P2 lipids extracted from *S. solfataricus* have been investigated in the present work by means of ESR spectroscopy of spin-labeled lipid probes. Phosphatidylcholines, *n*-PCSL, that are spin-labeled systematically throughout the acyl chain (at positions n = 5, 7, 10, 12, 14, and 16) are used to map out the transmembrane profiles of polarity and lipid chain flexibility. A comparison is made with similar measurements carried out on bilayer membranes of diphytanoyl phosphatidylcholine, which has methyl-branched chains, and also of the straight-chain reference lipid, dipalmitoyl phosphatidylcholine (see Figure 1).

MATERIALS AND METHODS

The P2-lipid fraction, composed of approximately 90% GDNT derivative and 10% GDGT (average molecular weight ca. 1870), was purified from the membrane of *S. solfataricus*, essentially as described by Gulik et al. (*7*). The synthetic lipid 1,2-dipalmitoyl-*sn*-glycero-3-phosphocholine (DPPC) was from Sigma (St. Louis, MO), and 1,2-diphytanoyl-*sn*-glycero-3-phosphocholine (DPhPC) was from Avanti Polar Lipids (Birmingham, AL). The spin-labeled lipids 1-palmitoyl-2-[*n*-(4,4-dimethyl-oxazolidin-*N*-oxyl)stearoyl]-*sn*-glycero-3-phosphatidylcholine (*n*-PCSL) with n = 5, 7, 10, 12, and 16 were also from Avanti, and the remaining *n*-PCSL was synthesized as described in Marsh and Watts (*18*). The reagent-grade salts for the 10 mM phosphate-buffered solution (PBS) at pH 7.5 were from Merck (Darmstadt, Germany). Distilled water was used throughout.

Preparation of Lipid Dispersions. P2 lipids were dissolved in $CHCl_3$/MeOH/H_2O with a volume ratio of 65:25:4. Multilamellar lipid dispersions were prepared by dissolving the lipids, together with 1 mol % of the required spin-labeled lipid in chloroform. The solvent was evaporated in a stream of dry nitrogen, and residual traces of the solvent were removed by placing the sample under vacuum overnight. The dried lipids were then dispersed in 10 mM PBS at pH 7.5 to a final lipid concentration of 25 mM by periodically vortexing and mixing at 60 °C for 40 min. The hydrated lipid dispersions were concentrated by centrifugation. Finally, the lipid dispersions were transferred to 1-mm (i.d.) 100 μL sample capillaries, flame-sealed, and incubated overnight at 4 °C before the running the ESR spectra.

ESR Measurements. ESR spectra were recorded with a Bruker ESP 300 spectrometer operating at 9 GHz (Bruker Biospin, Karlsruhe, Germany) and were digitized by using the spectrometer's built-in microcomputer with OS-9 compatible ESP 1600 spectral acquisition software. Sealed sample capillaries were inserted in a standard 4-mm i.d., quartz ESR tube that contained light silicone oil for thermal stability and were centered in the TE_{102} (ER 4201, Bruker) rectangular resonator. The sample temperature was controlled with a Bruker variable temperature controller, model ER-4111 VT (accuracy of ±0.5 °C). Conventional, first harmonic, in-phase absorption ESR spectra were recorded at a microwave power of 10 mW and with 100-kHz magnetic field modulation of amplitude 1 G peak-to-peak.

Spectra were analyzed in terms of the outer hyperfine splitting, $2A_{max}$, which is a useful empirical measure of the chain dynamics and ordering that is valid in both slow and fast motional regimes of nitroxide ESR spectroscopy (*19*, *20*). In the motional narrowing regime, at high temperature, A_{max} is equal to the parallel element, $A_{||}$, of the partially motionally averaged, axial hyperfine tensor. The perpendicular element, $A_{\perp}$, is derived from the separation, $2A_{min}$,

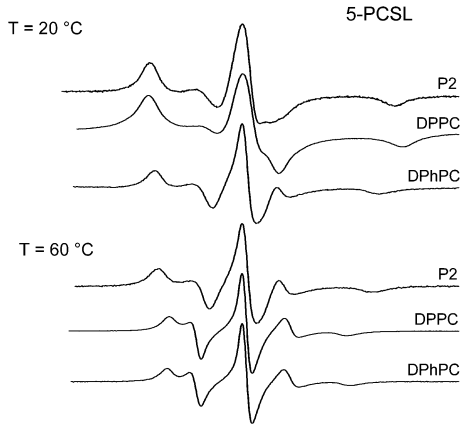

FIGURE 2: ESR spectra at 20 and 60 °C of 5-PCSL in aqueous dispersions of P2 lipids, DPPC and DPhPC. Total scan width = 100 G.

of the inner extrema, according to Schorn and Marsh (*21*)

$$A_{\perp}\,(\text{Gauss}) = A_{\min} + 1.32 + 1.86\log_{10}(1 - S_{\text{app}}) \quad \text{for } S_{\text{app}} \geq 0.45 \quad (1)$$

and

$$A_{\perp}\,(\text{Gauss}) = A_{\min} + 0.85 \quad \text{for } S_{\text{app}} < 0.45 \quad (2)$$

where $S_{\text{app}} = (A_{\max} - A_{\min})/[A_{zz} - 1/2(A_{xx} + A_{yy})]$ for a spin-label hyperfine tensor with Cartesian elements $(A_{xx}, A_{yy}, A_{zz}) = (5.9, 5.4, 32.9)$ Gauss.

The transmembrane polarity was then characterized by means of the isotropic ^{14}N-hyperfine coupling, A_o, (*22*) that is given by

$$A_o = 1/3(A_{||} + 2A_{\perp}) \quad (3)$$

for axially anisotropic spectra or simply by the hyperfine splitting in the case of isotropic spectra.

RESULTS AND DISCUSSION

Spin-label ESR measurements were carried out on the P2 tetraether, biphytanyl lipids in aqueous dispersion, over the temperature range of 10−80 °C. For comparison, similar measurements were performed on aqueous dispersions of the methyl-branched diphytanoyl lipid DPhPC and of the straight-chain, diacyl reference lipid DPPC. The temperature variation of the spectral anisotropy is closely related to structural and dynamical changes that occur in the lipid aggregates (*23*−*25*). Additionally, the isotropic hyperfine couplings (that are obtained from the spectra in the high-temperature regime) are sensitive to the local environmental polarity within the membrane (*26*, *27*) but are insensitive to the chain dynamics.

Temperature Dependence of Chain Mobility. ESR spectra of 5-PCSL in aqueous dispersions of P2, DPPC, and DPhPC lipids, at 20 and 60 °C, are shown in Figure 2. The ESR spectra of this spin label, which is located near the polar headgroup of the lipid chains, display an axial anisotropy that is characteristic of lamellar amphiphile assemblies.

At 20 °C, the spectrum of 5-PCSL in dispersions of the P2 lipids corresponds to rotational motion that is slow on the conventional spin-label time scale (correlation time ≥ 10 ns). It is somewhat similar to the spectrum of the same spin label in DPPC dispersions, which is in the $L_{\beta'}$ gel phase (i.e., below the chain-melting transition) at this temperature. In contrast, an axial line shape with a considerably lower degree of spectral anisotropy is found for 5-PCSL in dispersions of DPhPC at 20 °C, indicating that these lipids are already in the fluid membrane phase.

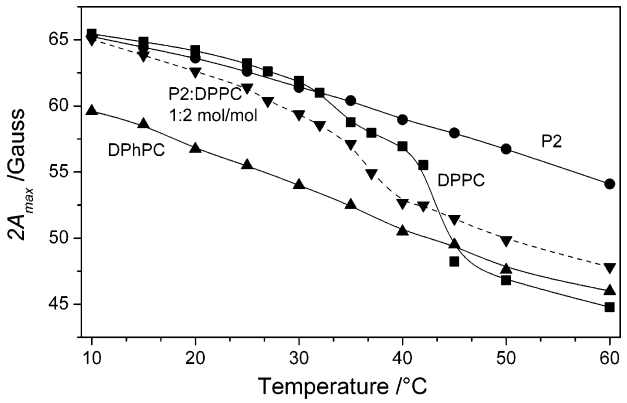

FIGURE 3: Temperature dependence of the outer hyperfine splitting, $2A_{\max}$, of 5-PCSL in aqueous dispersions of P2 lipids (●), DPPC (■), DPhPC (▲), and 1:2 P2/DPPC (mol/mol) mixture (▼, - - -).

Upon increasing the temperature to 60 °C, the total spectral range and anisotropy decreased markedly: to the greatest extent for DPPC dispersions, to a lesser extent for P2 dispersions, and to an even lower extent for DPhPC dispersions. All spectral line shapes are motionally narrowed, axially anisotropic, powder patterns as is expected for fluid, liquid-crystalline phases of aqueous lipid dispersions. The extent of motional narrowing (i.e., amplitude of rotational motion) is greatest for DPPC, somewhat less for DPhPC, and least for the P2 lipids. In addition, the spectral line widths are greater for the P2 lipids, indicating appreciably slower rotational motion than in bilayers of the two diacyl lipids. Upon going from low to high temperature, the chain dynamics change progressively from slow to intermediate motion in P2 lipids, from intermediate to rapid motion in DPhPC dispersions, and from slow to rapid motion in DPPC dispersions, on the conventional ESR time scale.

Figure 3 shows the temperature dependence of the outermost peak separation, $2A_{\max}$, of 5-PCSL in the three lipid dispersions. The well-known thermotropic phase behavior of DPPC bilayers is clearly identified, with a pretransition at ca. 32 °C and main, chain-melting transition at ca. 42−43 °C. In contrast, neither P2 nor DPhPC lipid dispersions exhibit thermotropic transitions between 10 and 60 °C. These results for DPhPC are consistent with the lack of any detectable calorimetric transition over the temperature range from −120 to 120 °C (*28*). A comparison with the results for DPPC above the chain-melting transition, in Figure 3, shows that the DPhPC dispersions are in a similar, fluid (L_{α}) phase at 45 °C and above. Because the same temperature dependence is maintained below 45 °C, the fluid phase of DPhPC bilayers must extend over the entire range from 10 to 80 °C. This is in agreement with conclusions reached earlier from the spectral line shapes in Figure 2. The temperature dependence of the outer hyperfine splitting of 5-PCSL in the P2-lipid dispersions is similar to that in DPhPC bilayers, although the absolute values of $2A_{\max}$ are considerably higher. This suggests that the unique cyclic bolaform structure of the P2 lipids limits *trans-gauche*

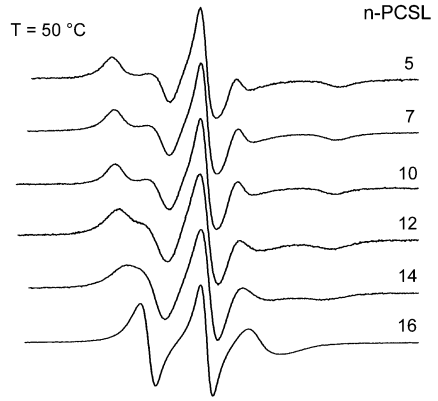

FIGURE 4: ESR spectra at 50 °C of different positional isomers of *n*-PCSL in aqueous dispersions of P2 lipids. Total scan width = 100 G.

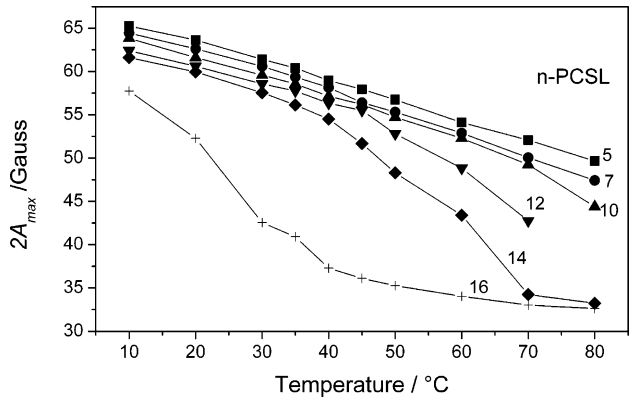

FIGURE 5: Temperature dependence of the outer hyperfine splitting, $2A_{max}$, from *n*-PCSL spin labels in aqueous dispersions of P2 lipids. $n = 5$ (■), 7 (●), 10 (▲), 12 (▼), 14 (◆), and 16 (+).

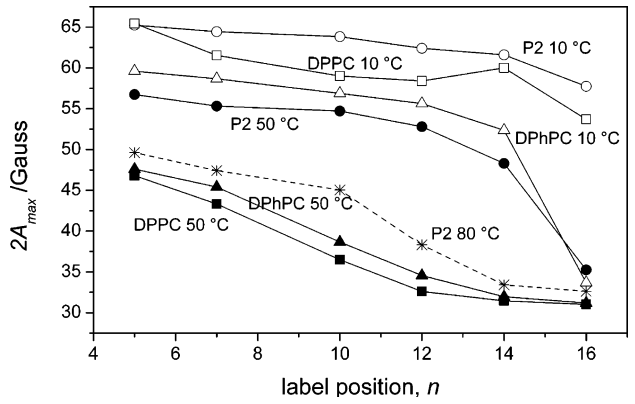

FIGURE 6: Outer hyperfine splitting, $2A_{max}$, as a function of the chain-labeling position, *n*, in aqueous dispersions of P2 lipids (○ and ●), DPPC (□ and ■), and DPhPC (△ and ▲) at 10 °C (○, □, and △) and 50 °C (●, ■, and ▲). The dashed line is for P2 lipids at 80 °C.

isomerism and reduces its rate, resulting in higher lipid order and slower chain motion in P2-lipid dispersions, as compared with diacyl lipids in conventional bilayer membranes.

Similar to the above, previous ESR results have indicated that, even at high temperature (80−85 °C), the motion of nitroxide stearic acids in aqueous dispersions of pure GDGT and pure GDNT lipids from *S. solfataricus* is restricted (*5*). Moreover, fluorescence data on bipolar tetraether liposomes composed of bolaform lipids from the thermoacidophilic archaeon *S. acidocaldarius* (the lipids of which are very similar in composition to P2) have shown that the hydrocarbon core is rather rigid and tightly packed below ≈50 °C, a temperature close to the minimum growth temperature (*12*). The generalized polarization of Laurdan fluorescence in giant unilamellar vesicles of lipids from *S. acidocaldarius* exhibits a small change at around 50 °C, which was attributed to a conformational change of the polar headgroups of the polar lipid fraction (*11*). This change correlates with a very small, low-enthalpy endothermic transition detected by differental scanning calorimetry of the GDNT lipid fraction (*4*). Above this temperature, the lipid mobility increases smoothly as required for the functionality of archaeal membranes.

Positional Dependence of Chain Mobility. Lipids spin-labeled at different positions, *n*, along the acyl chain (*n*-PCSL) were used to investigate the segmental lipid chain motion at different temperatures. Figure 4 shows the ESR spectra at 50 °C for each position of chain labeling in dispersions of the P2 lipids. For labels at positions C-5−C-10, the spectra are rather similar. Only for labels closer to the end of the chain, at positions C-12−C-16, does the spectral anisotropy decrease progressively down the chain. This is in contrast to the behavior of the same spin labels in fluid bilayers of diacyl lipids, for which the spectral anisotropy decreases continuously from the C-5 position onward (*29*, *30*).

Figure 5 gives the temperature dependence of the outer hyperfine splitting, $2A_{max}$, for each of the *n*-PCSL labels in dispersions of P2 lipids. Below 40 °C, the dependence on the chain position is even less than at 50 °C. Only the label at the C-16 position, close to the terminal methyl group, exhibits a very marked degree of motional averaging. Only at above 60 °C does a difference between all label positions finally begin to appear. This behavior is similar to that observed in a previous ESR study performed on aqueous dispersions of pure GDGT and pure GDNT lipids (*5*).

Figure 6 compares the dependences of $2A_{max}$ on the position, *n*, for the *n*-PCSL spin labels in dispersions of the P2 lipids with those of DPhPC and DPPC. Data are shown at 10 and 50 °C, where DPPC is in the gel and fluid phase, respectively. The characteristic chain flexibility gradient of diacyl lipids in fluid bilayers is evident for both DPhPC and DPPC at 50 °C. The value of $2A_{max}$ decreases continuously on going from the C-5 to C-12 position, and close to the terminal methyl end of the chain ($n = 14$ and 16), the motional averaging becomes complete. This behavior contrasts strongly with that at the same temperature in dispersions of the P2 lipids, which lack a bilayer midplane. For the bipolar lipids, the flexibility gradient at 50 °C is still severely restricted. The lipid chains are rather highly ordered along most of their length. The motional averaging that is seen at the C-14 and C-16 positions at this temperature most likely reflects the proximity to the terminal methyl group of the reporter spin label rather than an intrinsic property of the host lipid. Such an end effect is observed for short-chain spin labels in bilayer membranes of longer lipids (*31*).

Only at 80 °C does the flexibility profile of the *n*-PCSL spin labels in P2 lipids begin to approach that in the fluid phases of DPPC or DPhPC lipids at 50 °C. Chain flexibility is then evidenced by the progressive, although nonuniform, decrease of outer hyperfine splitting with the position in the chain of the diacyl lipid probes, in P2 lipids. Even at this

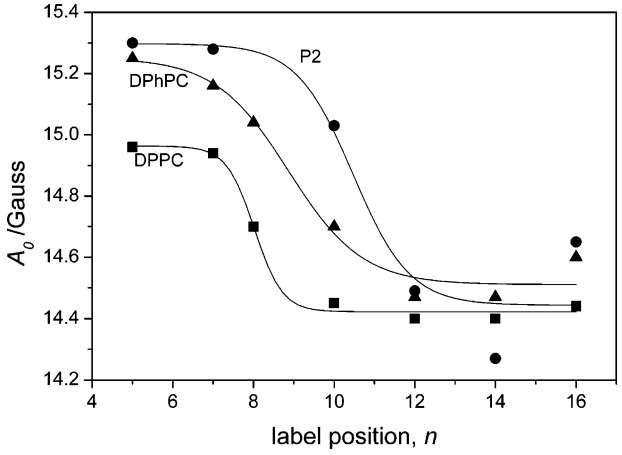

FIGURE 7: Positional dependence of the isotropic ^{14}N hyperfine couplings, A_o, of *n*-PCSL spin labels in aqueous dispersions of P2 lipids (●), DPPC (■), and DPhPC (▲). Solid lines are nonlinear least-squares fits of eq 4. For P2 lipids, the width of the sigmoid was maintained fixed during the fitting at $\lambda = 0.7$.

elevated temperature, however, the values of $2A_{max}$ are invariably somewhat larger than those for DPPC and DPhPC at much lower temperatures (i.e., 50 °C).

The spin-label ESR results indicate that the membrane of the P2 lipids is rigid and tightly packed. Only at an elevated temperature, close to that of the growth of the bacteria (about 80 °C), are the P2 lipids in a state comparable to the physiological state of normal bilayer lipids. The cyclic, bolaform, ether-linked structure allows a functional lipid membrane to withstand the extremes of high temperature and acidity to which *S. solfataricus* is exposed.

The molecular properties found here for P2 lamellae are shared by other tetraether membranes, which gain appreciable fluidity only for temperatures close to those of the growth (*12*). A significant feature in this regard is the hydrogen-bonding network at the polar/apolar interface (*10*). This explains the very low proton permeability across tetraether liposomal membranes (*13*, *14*) that support a large proton gradient across the membrane under physiological conditions.

Transmembrane Polarity Profiles. Figure 7 gives the dependence of the polarity-sensitive isotropic hyperfine couplings, A_o, on the position, *n*, of chain labeling for the *n*-PCSL spin labels in aqueous dispersions of P2 lipids and of DPhPC and DPPC. Determinations of A_o are made in the motional narrowing region, at high temperature, for which the isotropic coupling is equal to the trace of the anisotropic couplings $A_{||}$ and $A_{\perp}$ or, in the case of isotropic spectra for labels close to the chain end, is obtained from the baseline crossing.

The data for DPPC bilayers are in agreement with previous measurements and display the trough-like transmembrane polarity profile that is characteristic for bilayers of diacyl lipids (*22*). The positional dependence is fitted by the Boltzmann sigmoidal form

$$A_o(n) = \frac{A_{o,1} - A_{o,2}}{1 + e^{(n-n_o)/\lambda}} + A_{o,2} \qquad (4)$$

where $A_{o,1}$ and $A_{o,2}$ are the limiting values of A_o at the polar headgroup and terminal methyl ends of the spin-label chain, respectively, and λ is an exponential decay constant. The midpoint in the transition of the curve is specified by $n = n_o$.

For DPPC, the solid line in Figure 7 is given by eq 4 with $n_o = 8.0 \pm 0.1$ and $\lambda = 0.4 \pm 0.2$, which is reasonably close to the range of parameters determined previously (*22*). For DPhPC, the value of $n_o = 8.9 \pm 0.4$ is similar to that for DPPC, whereas for the P2 tetraether lipids, the fitted value of $n_o = 10.5 \pm 0.7$ is considerably larger. It is interesting to note that the thickness of the hydrocarbon region for fluid P2 lipids, $d_{HC} = 3.07$ nm (*7*), is appreciably greater than that for a DPPC bilayer, $d_{HC} = 2.85$ nm (*32*). Therefore, despite the difference in values of n_o, the width of the hydrophobic barrier may not be much smaller for P2 lipids than for DPPC. If a gradient of 0.11 nm/CH_2 is taken for the dependence of bilayer thickness on the lipid chain length (*32*), then the two are predicted to be rather similar.

To within experimental uncertainty, the values of A_o in the region of the membrane midplane (i.e., $A_{o,2}$) are rather similar for all three lipids, although a lower A_o value is obtained at the C-14 position for the P2 dispersions. This indicates that a region of reduced water penetration exists in the hydrocarbon region of the P2-lipid membranes as is found for DPPC, DPhPC, and other conventional cholesterol-free bilayer membranes (*22*). In combination with a similar width of the hydrophobic barrier, this implies that the water permeability of P2-lipid membranes will be comparable to (or less than) that of lipid bilayer membranes (*22*). In fact, the permeability coefficient, P_w, is determined both by the partition coefficient, $K_w(x)$, and also by the diffusion coefficient, $D_w(x)$, of water at position *x* in the membrane

$$\frac{1}{P_w} = \int_{-d/2}^{d/2} \frac{dx}{K_w(x)D_w(x)} \qquad (5)$$

where *d* is the membrane thickness. Whereas the partition coefficient is determined by the polarity profile, the diffusion coefficient will depend upon the lipid chain flexibility profile. Because the chain flexibility is reduced considerably for the P2 lipids, it is expected that the overall water permeability will thus be appreciably lower for membranes of these lipids than for normal bilayer membranes composed of diacyl lipids.

The values of A_o in the chain regions close to the lipid headgroups (i.e., $A_{o,1}$) are significantly greater in the P2-lipid membranes than in DPPC bilayers. This enhanced penetration of water in the upper parts of the chains is attributed to the branched methyl groups in the biphytanyl chains of the P2 lipids, because it is a feature shared with diphytanoyl PC bilayers (see Figure 7). Nonetheless, as already noted, the height of the hydrophobic barrier is at least as great as that in bilayers of saturated-chain lipids.

Bipolar Lipids Mixed with Phosphatidylcholine. Admixture of bisubstituted *S. solfataricus* lipids with diacyl phosphatidylcholine has been found to stabilize liposomes against Ca^{2+}- or poly(ethylene glycol)-induced fusion (*9*). Therefore, it is of considerable interest to investigate the lipid chain mobility in P2/DPPC mixtures. A 1:2 (mol/mol) mixture is used because this was found to have the greatest stabilizing effect (*8*).

Throughout the temperature range from 10 to 80 °C, the ESR spectra of 5-PCSL in dispersions of the 1:2 (mol/mol) mixture of P2/DPPC lipids consist of a single, axially

anisotropic component (spectra not shown). This indicates that the two lipids mix well at these proportions. The dashed line in Figure 3 depicts the temperature dependence of the outer hyperfine splitting, $2A_{max}$, of 5-PCSL in the lipid mixture. Below 40 °C, the temperature dependence is similar to that in the gel phase of DPPC, although the absolute values of $2A_{max}$ are smaller and the pretransition is less obvious. The discontinuity in $2A_{max}$ at the chain-melting transition of DPPC is less abrupt and considerably attenuated in the 1:2 P2/DPPC (mol/mol) mixture. Above 40 °C, the values of $2A_{max}$ in the mixture are intermediate between those of the P2 lipids and DPPC alone. Thus, the bipolar lipids incorporate well into both gel and liquid-crystalline phases of DPPC. The stabilizing effect of P2 lipids in the fluid phase correlates with the pronounced increase in chain order, which arises because the bisubstituted lipids are firmly anchored at the polar−apolar interfaces of both bilayer leaflets.

CONCLUSIONS

The ESR results using chain-labeled lipids indicate that the bolaform P2 lipids, when fully hydrated in buffer, form membranes whose chains do not undergo a melting transition and are more ordered and less flexible than those of fluid bilayer lipids at the same temperature. Only at elevated temperatures (around 80 °C) does the flexibility of the chain environment in P2-lipid membranes approach that in bilayers of diacyl lipids at their respective ambient or physiological temperatures. At such extreme temperatures, conventional bilayer membranes would be highly expanded relative to their normal state, which could compromise their barrier properties and the stability of embedded membrane proteins. P2-lipid dispersions maintain the rigidity of the plasma membrane of *S. solfataricus* needed to tolerate extreme environmental growth conditions and acquire appreciable fluidity needed for functionality at temperatures close to that of minimum growth.

Although composed of only a single monolayer constituted by methyl-branched chains, the height of the hydrophobic barrier offered by P2-lipid membranes is similar to (or greater than) that in normal fluid bilayer membranes. Also, the width of this permeability barrier is comparable to that in conventional fluid DPPC bilayers.

The tetraether P2 lipids mix well with diacyl DPPC bilayer lipids, at a mole ratio of 1:2. In doing so, the P2 lipids confer on the DPPC lipids a chain ordering and stabilization that is intermediate between that of DPPC and P2 lipids alone. Liposome stability is also related to the bipolar nature of P2, which does not support peeling of one monolayer of the liposomal membrane from the other. In fact, fusion mediated by calcium and by the powerful fusogenic glycoprotein influenza virus, hemagglutinin, is inhibited (*9*, *15*). This point is of practical relevance in that bipolar tetraether P2 lipids might be used to form liposomes of high structural and thermal stability, which could be suitable for application in different biotechnological areas.

ACKNOWLEDGMENT

We thank Dr. Annalisa Relini for helpful discussions, Frau B. Angerstein for the synthesis of spin-labeled lipids, and Mr. E. Pagnotta for purification of the P2 lipids. R. B., L. S., and D. M. are members of the European COST D22 Action.

REFERENCES

1. De Rosa, M., and Gambacorta, A. (1988) The lipids of archaebacteria, *Prog. Lipid Res. 27*, 153−175.
2. Kates, M. (1992) Archaebacterial lipids−Structure, biosynthesis, and function, *Biochem. Soc. Symp. 58*, 51−72.
3. Gambacorta, A., Gliozzi, A., and De Rosa, M. (1995) Archaeal lipids and their biotechnological applications, *World J. Microbiol. Biotechnol. 11*, 115−131.
4. Gliozzi, A., Paoli, G., De Rosa, M., and Gambacorta, A. (1983) Effect of isoprenoid cyclization on the transition temperature of lipids in thermophilic archaebacteria, *Biochim. Biophys. Acta 735*, 234−242.
5. Bruno, S., Cannistraro, S., Gliozzi, A., De Rosa, M., and Gambacorta, A. (1985) A spin label ESR and saturation transfer−ESR study of archaeabacteria bipolar lipids, *Eur. Biophys. J. 13*, 67−76.
6. De Rosa, M., Gambacorta, A., and Ghiozzi, A. (1986) Structure, biosynthesis, and physicochemical properties of archaebacterial lipids, *Microbiol. Rev. 50*, 70−80.
7. Gulik, A., Luzzati, V., De Rosa, M., and Gambacorta, A. (1988) Tetraether lipid components from a thermoacidophilic archaebacterium−Chemical structure and physical polymorphism, *J. Mol. Biol. 201*, 429−435.
8. Fan, Q., Relini, A., Cassinadri, D., Gambacorta, A., and Ghiozzi, A. (1995) Stability against temperature and external agents of vesicles compared of archaeal bolaform lipids and egg PC, *Biochim. Biophys. Acta 1240*, 83−88.
9. Relini, A., Cassinadri, D., Fan, Q., Gulik, A., Mirghani, Z., De Rosa, M., and Ghiozzi, A. (1996) Effect of physical constraints on the mechanisms of membrane fusion: Bolaform lipid vesicles as model systems, *Biophys. J. 71*, 1789−1795.
10. Vilalta, I., Gliozzi, A., and Pratz, M. (1996) Interfacial air/water proton conduction from long distances by *Sulfolobus solfataricus* archaeal bolaform lipids, *Eur. J. Biochem. 240*, 181−190.
11. Bagatolli, L., Gratton, E., Khan, T. K., and Chong, P. L.-G. (2000) Two photon fluorescence microscopy studies of bipolar tetraether giant liposomes from thermoacidophilic archaebacteria, *Sulfolobus solfataricus*, *Biophys. J. 79*, 416−425.
12. Khan, T. K., and Chong, P. L.-G. (2000) Studies of archaebacterial bipolar tetraether lipids by perylene fluorescence, *Biophys. J. 813*, 1390−1399.
13. Mathai, J., Sprott, G. D., and Zeidel, M. L. (2001) Molecular mechanism of water and solute transport across archaebacterial lipid membranes, *J. Biol. Chem. 276*, 27266−27271.
14. Komatsu, H., and Chong P. L.-G. (1998). Low permeability of liposomal membranes composed of bipolar tetraether lipids from thermophilic archaebacterium *Sulfolobus acidocaldarius*, *Biochemistry 37*, 107−115.
15. Bailey A., Zhukovsky M., Gliozzi A., and Chernomordik L. V. (2005) Liposome composition effects on lipid mixing between cells expressing influenza virus hemagglutinin and bound liposomes, *Arch. Biochem. Biophys. 439*, 211−221.
16. Gliozzi, A., and Relini, A. (1996) Lipid vescicles as model systems for Archaea membranes, in *Handbook of Nonmedical Applications of Liposomes* (Lasic, D. D., and Barenholz, Y., Eds.) Vol. 2, pp 329−348, CRC Press, Boca Raton, FL.
17. Gliozzi, A., Relini, A., and Chong, P. L.-G. (2002) Structure and permeability properties of biomimetic membranes of bolaform archaeal tetraether lipids, *J. Membr. Sci. 206*, 131−147.
18. Marsh, D., and Watts, A. (1982) Spin-labeling and lipid−protein interactions in membranes, in *Lipid−Protein Interactions* (Jost, P. C., and Griffith, O. H., Eds.) Vol. 2, pp 53−126, Wiley-Interscience, New York.
19. Rama Krishna, Y. V. S., and Marsh, D. (1990) Spin label ESR and ^{31}P NMR studies of the cubic and inverted hexagonal phases of dimyristoylphosphatidylcholine/myristic acid (1:2, mol/mol) mixtures, *Biochim. Biophys. Acta 1024*, 89−94.
20. Schorn, K., and Marsh, D. (1996) Lipid chain dynamics and molecular location of diacylglycerol in hydrated binary mixtures with phosphatidylcholine: Spin label ESR studies, *Biochemistry 35*, 3831−3836.
21. Schorn, K., and Marsh, D. (1997) Extracting order parameters from powder ESR lineshapes for spin-labelled lipids in membranes, *Spectrochim. Acta, Part A 53*, 2235−2240.

22. Marsh, D. (2001) Polarity and permeation profiles in lipid membranes, *Proc. Natl. Acad. Sci. U.S.A. 98*, 7777−7782.
23. Freed, J. H. (1976) Theory of slowly tumbling ESR spectra for nitroxides, in *Spin Labeling, Theory, and Applications* (Berliner, L. J., Ed.) pp 53−132, Academic Press, New York.
24. Marsh, D. (1981) Electron spin resonance: Spin labels, in *Membrane Spectroscopy. Molecular Biology, Biochemistry, and Biophysics* (Grell, E., Ed.) pp 51−142, Springer-Verlag, New York.
25. Marsh, D., and Horváth, L. I. (1989) Spin-label studies of the structure and dynamics of lipids and proteins in membranes, in *Advanced ESR. Applications in Biology and Biochemistry* (Hoff, A. J., Ed.) pp 707−752, Elsevier, Amsterdam, The Netherlands.
26. Marsh, D. (2002) Polarity contributions to hyperfine splittings of hydrogen-bonded nitroxides—The microenvironment of spin labels, *J. Magn. Reson. 157*, 114−118.
27. Marsh, D. (2002) Membrane water-penetration profiles from spin labels, *Eur. Biophys. J. 31*, 559−562.
28. Lindsey, H., Petersen, N. O., and Chan, S. I. (1979) Physicochemical characterization of 1,2-diphytanoyl-*sn*-glycero-3-phosphocholine in model membrane systems, *Biochim. Biophys. Acta 555*, 147−167.
29. Sankaram, M. B., Brophy, P. J., and Marsh, D. (1989) Spin label ESR studies on the interaction of bovine spinal cord myelin basic protein with dimyristoylphosphatidylglycerol dispersions, *Biochemistry 28*, 9685−9691.
30. Pérez-Gil, J., Casals, C., and Marsh, D. (1995) Interactions of hydrophobic lung surfactant proteins SP-B and SP-C with dipalmitoylphosphatidylcholine and dipalmitoylphosphatidylglycerol bilayers studied by electron spin resonance spectroscopy, *Biochemistry 34*, 3964−3971.
31. Reboiras, M. D., and Marsh, D. (1991) ESR studies on the influence of chainlength on the segmental motion of spin-labelled fatty acids in dimyristoylphosphatidylcholine bilayers, *Biochim. Biophys. Acta 1063*, 259−264.
32. Nagle, J. F., and Tristram-Nagle, S. (2000) Structure of lipid bilayers, *Biochim. Biophys. Acta 1469*, 159−195.

BI051101I